Journal of Venom Research ISSN: 2044-0324 J Venom Res, 2020, Vol 10, 23-29

RESEARCH ARTICLE

Snake C-type lectin-like proteins inhibit nicotinic acetylcholine receptors

Elena V Kryukova[1], Catherine A Vulfius[2], Rustam H Ziganshin[1], Tatyana V Andreeva[1], Vladislav G Starkov[1], Victor I Tsetlin[1], Yuri N Utkin[1,*]

[1]Shemyakin-Ovchinnikov Institute of Bioorganic Chemistry Russian Academy of Sciences, ul. Miklukho-Maklaya 16/10, Moscow 117997, Russia

[2]Institute of Cell Biophysics Russian Academy of Sciences, 3 Institutskaya Street, Pushchino Moscow region, 142290, Russia

***Correspondence to:** Yuri Utkin, E-mail: utkin@ibch.ru; yutkin@yandex.ru, Tel/Fax: +74953366522

Received: 30 April 2020 | **Revised:** 02 July 2020 | **Accepted:** 06 July 2020 | **Published:** 06 July 2020

ABSTRACT

Venoms of viperid snakes affect mostly hemostasis, while C-type lectin-like proteins (CTLPs), one of the main components of viperid venoms, act as anticoagulants, procoagulants, or agonists/antagonists of platelet activation. However, we have shown earlier that CTLPs from the saw-scaled viper *Echis multisquamatus*, called emunarecins EM1 and EM2, were able to inhibit nicotinic acetylcholine receptors (nAChRs) in neurons of a pond snail (*Lymnaea stagnalis*). Here we analysed the structure of the emunarecins by mass spectrometry and report that EM1 and EM2 inhibit fluorescent α-bungarotoxin binding to both muscle-type nAChRs from *Torpedo californica* and human neuronal α7 nAChRs. EM1 at 23μM and EM2 at 9μM almost completely prevented fluorecsent α-bungarotoxin binding to muscle-type nAChRs. Interaction with human neuronal α7 nAChR was weaker; EM1 at the concentration of 23μM blocked the α-bungarotoxin binding only by about 40% and EM2 at 9μM by about 20%. The efficiency of the EM2 interaction with nAChRs was comparable to that of a non-conventional toxin, WTX, from Naja kaouthia cobra venom. Together with the data obtained earlier, these results show that CTLPs may represent new nAChR ligands.

KEYWORDS: α-bungarotoxin, C-type lectin-like protein, nicotinic acetylcholine receptor, saw-scaled viper, snake, venom

INTRODUCTION

The main task of the venom is to immobilize prey. During their evolution, snakes acquired venoms that affect two main vitally important systems in prey organisms – the nervous and the cardiovascular systems. Depending on the affected system, the venom can be either classified as neurotoxic or hemotoxic. The venoms of the elapid snakes are mostly neurotoxic, while those of the Viperidae are generally hemotoxic. However, some elapid venoms manifest hemotoxicity, while viperid venoms exhibit neurotoxicity, and several neurotoxic components have been isolated from viperid venoms. The best known examples are the neurotoxic dimeric phospholipases A_2 crotoxin and vipoxin isolated from the venoms of the South American rattlesnake *Crotalus durissus terrificus* and the Bulgarian viper *Vipera ammodytes meridionalis*, respectively (Sampaio et al, 2010; Petrova et al, 2012). These toxins act presynaptically at the neuromuscular junction, producing muscle paralysis (Petrova et al, 2012; Cavalcante et al, 2017). It should be mentioned that in snake venoms there are many other toxins acting postsynaptically by inhibiting nicotinic acetylcholine receptors (nAChRs). These receptors are the

main target of α-neurotoxins, potent nAChR inhibitors from elapid venoms.

In our earlier works, we showed that crotoxin and other phospholipases A_2 bind to and block different nAChR subtypes (Vulfius et al, 2014; Vulfius et al, 2017). Furthermore, a peptide neurotoxin azemiopsin, a quite potent competitive blocker of nAChRs, was isolated from the Feae's viper (*Azemiops feae*) venom (Utkin at al, 2012), and peptides inhibiting these receptors non-competitively were isolated from the venom of the puff adder *Bitis arietans* (Vulfius et al, 2016). Two neurotoxic peptides, waglerins I and II, were purified from the venom of the Asian pit-viper *Trimeresurus wagleri* (Weinstein et al, 1991). These data indicate that toxins directed against nAChRs are not so rare in the venoms of viperid snakes. Recently, we have studied the venom of the saw-scaled viper (*Echis multisquamatus*) and found that some proteins of this venom are capable of inhibiting nAChRs in neurons of a pond snail (*Lymnaea stagnalis*) (Vulfius et al, 2015). Basing on the preliminary data we have suggested that these proteins, which were called emunarecins, may be C-type lectin-like proteins (CTLPs). In this paper we describe the detailed characterization of emunarecins and show that CTLPs from *E. multisquamatus* inhibit both α7 and muscle type nAChRs, manifesting the higher affinity to the muscle type receptor. This is the first indication of nAChRs being inhibited by CTLPs.

MATERIALS AND METHODS

Materials

All salts obtained from local suppliers were of analytical grade or higher. Tween-20 was from Sigma Aldrich (St Louis, MO, USA). α-Bungarotoxin (α-Bgt) labelled with Alexa-488 (Alexa-Bgt) was purchased from Thermo Fisher Scientific (Waltham, MA, USA). GH_4C_1 cells transfected with hα7 nAChR cDNA were a gift of the Eli Lilly Co (London, UK). Muscle-type nAChR-enriched membranes from the electric organs of *Torpedo californica* were kindly provided by Professor F Hucho (Free University of Berlin, Germany).

Venom fractionation

The venom of the saw-scaled viper *E. multisquamatus* was fractionated as described (Vulfius et al, 2015). In brief, gel filtration was performed on a Superdex™ 75 column (10x300mm, Cytiva, Marlborough, MA, USA), equilibrated with 0.1M ammonium acetate (pH 6.2). The eluting proteins were detected by absorbance at 280nm. After analysis for the capacity to inhibit acetylcholine elicited current in *Lymnaea* neurons, the active fraction was separated further by anion-exchange chromatography on a Mono Q column (5 x 50mm, Cytiva, Marlborough, MA, USA) with a gradient of sodium chloride concentration in 5mM Tris-HCl buffer (pH 7.5). After screening for inhibitory activity on *Lymnaea* neurons, active fractions were desalted on a Superdex™ 75 column equilibrated in 0.1M ammonium acetate (pH 6.2) and freeze dried twice. The proteins obtained were used for further study.

Reduction and pyridylethylation

Reduction and pyridylethylation were performed as previously described in Ramazanova et al (2008).

Mass spectrometry analysis

For mass spectrometry measurements, the pyridylethylated proteins were digested with trypsin at a 1:100 (w/w) ratio overnight at 37°C. Desalting of peptides was carried out using SDB-RPS StageTips that were prepared as described earlier (Rappsilber et al, 2007). After overnight digestion, peptide solution was acidified by equal volume of 2% (v/v) TFA and peptides were loaded on StageTip by centrifugation at 200x*g*. StageTip was washed by 50µl 0.2% (v/v) TFA and peptides were eluted by 50µl 50% (v/v) acetonitrile, 0.1% (v/v) TFA, lyophilized and stored at -80 °C. Before analyses peptides were dissolved in 20µl of 2% (v/v) acetonitrile, 0.1% (v/v) TFA and sonicated for 2min. For LC-MS analyses, peptides were separated on a 50-cm 75µm inner diameter column packed in-house with Aeris Peptide XB-C18 2.6µm resin (Phenomenex). Reverse-phase chromatography was performed with an Ultimate 3000 Nano LC System (Thermo Fisher Scientific), which was coupled to a Q Exactive HF benchtop Orbitrap mass spectrometer (Thermo Fisher Scientific) via a nanoelectrospray source (Thermo Fisher Scientific). The mobile phases were: A) 0.1% (v/v) formic acid in H_2O and B) 0.1% (v/v) formic acid, 80% (v/v) acetonitrile, 19.9% (v/v) H_2O. Samples were loaded onto a trapping column (100µm internal diameter, 20mm length, packed in-house with Aeris Peptide XB-C18 2.6µm resin (Phenomenex)) in mobile phase A at flow rate 5µl/min for 5min and eluted with a linear gradient of mobile phase B (5-45% (v/v) B in 60min at a flow rate of 350nl/min. Column temperature was kept at 40 °C. Peptides were analyzed on the Q Exactive HF benchtop Orbitrap mass spectrometer (Thermo Fisher Scientific), with one full scan (300–1,400*m/z*, *R* = 60,000 at 200*m/z*) at an AGC target of 3e6 ions, followed by up to 15 data-dependent MS/MS scans with higher-energy collisional dissociation (HCD) (target 1e5 ions, max ion fill time 30ms, isolation window 1.2 m/z, normalized collision energy (NCE) 28%, underfill ratio 2%), detected in the Orbitrap (*R* = 15,000 at fixed first mass 100 *m/z*). Other settings: charge exclusion - unassigned, 1, >6; peptide match – preferred; exclude isotopes – on; dynamic exclusion - 30s was enabled. MS raw files were analyzed by PEAKS Studio 8.5 (Bioinformatics Solutions Inc) (Ma et al, 2003) and peak lists were searched against Serpentes Uniprot-Tremble FASTA (canonical and isoform) database version of May 2018 (144954 entries) with cysteine pyridylethylation as a fixed modification and methionine oxidation and asparagine and glutamine deamidation as variable modifications. Enzyme specificity in the database search was set to trypsin with semi-specific digest mode. False discovery rate was set to 0.01 for peptide-spectrum matches and was determined by searching a reverse database. Peptide identification was performed with an allowed initial precursor mass deviation up to 10ppm, and an allowed fragment mass deviation 0.05Da.

Competitive fluorescence analysis

For competition binding assays, suspensions of nAChR-rich membranes from *T. californica* ray electric organ (0.31nM α-Bgt binding sites) or human α7 nAChR transfected GH_4C_1 cells (0.25nM α-Bgt binding sites) in phosphate buffered saline (mM: NaCl 137, KCl 2, KH_2PO_4 1.47, Na_2HPO_4 8.1; pH 7.4) containing 0.1% (v/v) Tween-20 (binding buffer) were incubated for 1hr with varying concentrations of emunare-

cins (from 1 to 23μM) in Falcon 96-well round-bottom plate (MICROTEST TM U-Bottom, Thomas Scientific, Swedesboro, NJ USA) in total volume of 100μl. After that, 20μl of Alexa-Bgt solution was added to the final concentration of 0.29nM, and the mixture was incubated for 5min more. Nonspecific binding was determined by preliminary incubation of the preparations with 100nM α-cobratoxin. The membrane and cell suspensions were applied to glass GF/C filters (Whatman, Little Chalfont, UK) presoaked in 0.5% (v/v) polyethylenimine, and the unbound Alexa-Bgt was removed from the filter by washing (3 × 0.2ml) with cold binding buffer. The amount of the bound Alexa-Bgt was measured by FFM-01 plate fluorometer (OOO Kortek, Moscow, Russia) using excitation wavelength at 482nm and emission at 538nm. Each experiment was done in quadruplicate. The data obtained were analyzed using OriginPro 7.5 program (OriginLab, Northampton, MA, USA).

Electrophysiological experiments

Experiments were performed on identified giant neurons isolated from the *Lymnaea* right or left parietal ganglia (RPV2,3, LP1,2,3) after mild digestion with Pronase E as described (Vulfius et al, 2005). Neurons were internally perfused with the solution containing (in mM): CsCl 95, $CaCl_2$ 0.3, EGTA 2, HEPES 10, pH 7.2 and voltage-clamped at -70mV. Constant flow of the external solution (in mM: NaCl 88, KCl 1.6, $CaCl_2$ 4, $MgCl_2$ 1.5, Trizma-HCl 4, pH 7.6) was maintained, except for the periods of agonist application or neuron incubation with EM1. Cytisine was applied on the whole cell surface using 4s pulses with intervals not less than 6min. Agonist-induced currents were monitored and digitized with a patch-clamp amplifier AM Systems (USA), the data acquisition was performed using Digidata 1200 B interface and pClamp6 software (Axon Instruments Inc., USA). Peak currents induced by cytisine at different concentrations in control and under EM1 action were normalized to the maximal current in response to a saturating cytisine concentration in control. The type of EM1 antagonism was determined according to the change of normalized current dependence on cytisine concentration in the same experiment. EM1 was used at a concentration of 100μg/ml that is close to IC_{50}.

RESULTS AND DISCUSSION

During our search for neurotoxins in viper venoms we found that the venom of the saw-scaled viper *E. multisquamatus* was able to inhibit nAChRs in *Lymnaea* identified neurons (Gorbacheva et al, 2008). These neuronal nAChRs are similar to the mammalian α7 nAChRs in sensitivity to some specific antagonists, which is why they were used by us as a model for a search of α7 active ligands. To isolate an active toxin, the crude venom was separated by gel-filtration and the fractions obtained were screened for the capacity to block *Lymnaea* nAChRs. The fraction manifesting the highest activity was further separated by anion exchange chromatography and the fractions obtained were again tested for inhibition of nAChR. Fractions demonstrating inhibitory activity on *Lymnaea* nAChR were called emunarecins 1 and 2 (EM1 and EM2, from ***E**chis **mu**ltisquamatus* **n**icotinic **a**cetylcholine **rec**eptor **in**hibitor) (Vulfius et al, 2015) and were used for further study.

Earlier we have shown (Vulfius et al, 2015) that, according to the gel filtration data, EM1 is a mixture of products with apparent molecular masses of approximately 70 and 160kDa, whereas EM2 has a molecular mass of approximately 160kDa. However, PAGE results showed that EM1 under nonreducing conditions displayed two major bands with apparent molecular masses of approximately 27 and 50kDa, while under reducing conditions, EM1 was divided into two very close subunits with apparent molecular masses of approximately 13kDa. PAGE analysis of EM2 under nonreducing conditions revealed a major band with a molecular mass of 120kDa and a minor band with a molecular mass of approximately 27kDa. However, under reducing conditions, EM2 yielded two subunits with molecular masses of approximately 18 and 13kDa. Based on these data we have suggested that emunarecins may represent CTLPs. It should be noted that snake venom CTLPs are heterodimers composed of homologous α and β subunits with molecular masses of 14-16kDa and 13-15kDa, respectively (Arlinghaus and Eble, 2012). These heterodimers can form multimers resulting in αβ, $(αβ)_2$, $(αβ)_4$ and more complex structures (Arlinghaus and Eble, 2012). That is what we observed for EM1 and EM2.

To confirm the data obtained earlier, EM1 and EM2 were analyzed by mass spectrometry. The isolated proteins were digested with trypsin and the digests obtained were analyzed by LC-MS/MS. The results showed that in EM1 one of the subunits was almost identical to α subunit of Snaclec EMS16 from *E. multisquamatus*. The amino acid sequences of EM1 subunit and α subunit of Snaclec EMS16 possessed 92% of identical amino acid residues (Figure 1A). Other EM1 polypeptide chain manifested homology to P-III metalloproteinases from the venoms of snakes of the *Echis* genus. The percent of the identical residues varied from 30 to 50% depending on the *Echis* species. Identical residues are concentrated mainly in several areas, mostly in the C-terminal fragment of about 150 amino acid residues. It was noted above that during electrophoresis under reducing conditions, EM1 gives two bands corresponding to polypeptides with molecular masses of about 13kDa. However, the identified metalloproteinases have much larger masses. Since we did not take special precautions to prevent autolysis in preparing the samples, it is quite possible that degradation of high molecular weight metalloproteinases with the formation of shorter polypeptides took place. Autolysis is a well-known phenomenon for snake venom metalloproteinases (Deshimaru et al, 2005; Van de Velde et al, 2018). It should be noted that earlier carinactivase-1 and multactivase, heterotrimeric complexes consisting of PIII metalloproteinase heavy chain and two light chains with features characteristic of CTLPs, were isolated from the venom of *E. carinatus* and *E. multisquamatus*, respectively (Yamada et al, 1996; Yamada and Morita, 1997). The transcripts encoding similar proteins were identified in the venom gland transcriptomes of *E. ocellatus, E. coloratus* and *E. c. sochureki* (Casewell et al, 2009). The complete amino acid sequences for multactivase is not known; however, based on the above data we can conclude that EM1 is a multimeric protein similar to multactivase and includes a metalloproteinase and a CTLP.

Somewhat different results were obtained after MS analysis of EM2. Similarly to EM1, one of EM2 subunits was

A

```
SLA_ECHML
MGRFISVSFGLLVVFLSLSGTGADFDCPSDWTAYDQHCYLAIGEPQNWYEAERFCTEQAK     60
DGHLVSIQSREEGNFVAQLVSGFMHRSEIYVWIGLRDRREEQQCNPEWNDGSKIIYVNWK     120
EGESKMCQGLTKWTNFHDWNNINCEDLYPFVCKFSAV  157
```

B

```
SLA_ECHML       MGRFISVSFGLLVVFLSLSGTGADFDCPSDWTAYDQHCYLAIGEPQNWYEAERFCTEQAK     60
SL3_ECHCS       WGDSSSSASACWSCSSPLSGTEAGVCCPLGWSGYDQNCYKAFEELMNWADAEKFCTQQHK     60

SLA_ECHML       DGHLVSIQSREEGNFVAQLVSGFMHRSEIYVWIGLRDRREEQQCNPEWNDGSKIIYVNWK     120
SL3_ECHCS       GSHLVSLHNIAEADFVVKKIVSVLKDG--VIWMGLNDVW--NECNWGWTDGAQLDYKAWN     116

SLA_ECHML       EGESKMCQGLTKWTNFHDWNNINCEDLYPFVCKFSAV    157
SL3_ECHCS       VESNCFI----FKTAENHWSRTDCSGTHSFVCKSPA-    148
```

Figure 1. Amino acid sequences of CTLP subunits to which EM1 and EM2 demonstrated homology. Signal peptides are shown in italics. SLA_ECHML is CTLP EMS16 subunit α from *E. multisquamatus*, SL3_ECHCS – CTLP snaclec 3 from *E. carinatus sochureki*. The underlined sequences were identified by mass spectrometry in EM1 (**A**) and EM2 (**B**). The alignment was done using CLUSTAL O(1.2.4) multiple sequence alignment tool (Madeira et al, 2019).

homologous to α subunit of Snaclec EMS16 from *E. multisquamatus*, 92% of amino acid residues being identical in both polypeptides. Other EM2 subunit was almost identical to Snaclec 3 from *E. carinatus sochureki*; in these two polypeptides 96% of amino acid residues were identical (Figure 1B). Compared to other heterodimer CTLPs, Snaclec 3 shows greater sequence similarity to the β than α subunits. Only a limited number of the tryptic peptides assigned to metalloproteinases were found. Thus, we conclude that EM2 is a typical CTLP comprising α and β subunits.

We further studied the interaction of EM1 and EM2 with the muscle type nAChR from *T. californica* electric organ and human neuronal receptor of α7 subtype using fluorescently labeled α-bungarotoxin Alexa-Bgt. In the experiments on *Torpedo* nAChR, EM1 showed a good affinity, leaving only about 35% Alexa-Bgt bound to the receptor at concentration of 1.6mg/ml, which corresponds to a maximum of 23μM, if the molecular mass for EM1 is taken as 70kDa (Figure 2A). The affinity of EM2 was even higher; at its concentration of 9μM, only 2% of Alexa-Bgt remained bound to nAChR (Figure 2A). Competition of toxins with Alexa-Bgt for binding to neuronal α7 nAChR was much weaker (Figure 2B). At the concentration of 23μM, EM1 left about 60% of α-bungarotoxin bound to the receptor, and at the concentration of 9μM, EM2 left about 80% of Alexa-Bgt bound to α7 nAChR (Figure 2B).

As was mentioned earlier, the biological activity of emunarecins was determined in electrophysiological experiments, which showed that the toxins inhibited currents induced by nAChR agonists (acetylcholine and cytisine) in *Lymnaea* neurons (Vulfius et al, 2015). The chloride-conducting *Lymnaea* nAChRs are similar to cation-conducting vertebrate neuronal nAChRs of the α7 subtype in interaction with various specific antagonists (α-cobratoxin, α-conotoxin ImI) and agonists (choline, cytisine) (Vulfius et al, 2001, 2005, 2014), but are not identical. On this *Lymnaea* nAChR, both emunarecins showed comparatively high activity, the IC_{50} for EM2 being 248μg/ml (1.55μM) and for EM1 being 122μg/ml. The binding was reversible and responses were recovered completely after EM1 washing out (Figure 3A). To determine if *Lymnaea* nAChR inhibition by emunarecins is competitive or noncompetitive, we analyzed the effect of EM1 on the currents elicited by cytisine at different concentrations (including the saturating ones). The currents elicited by cytisine were recorded before and after incubation

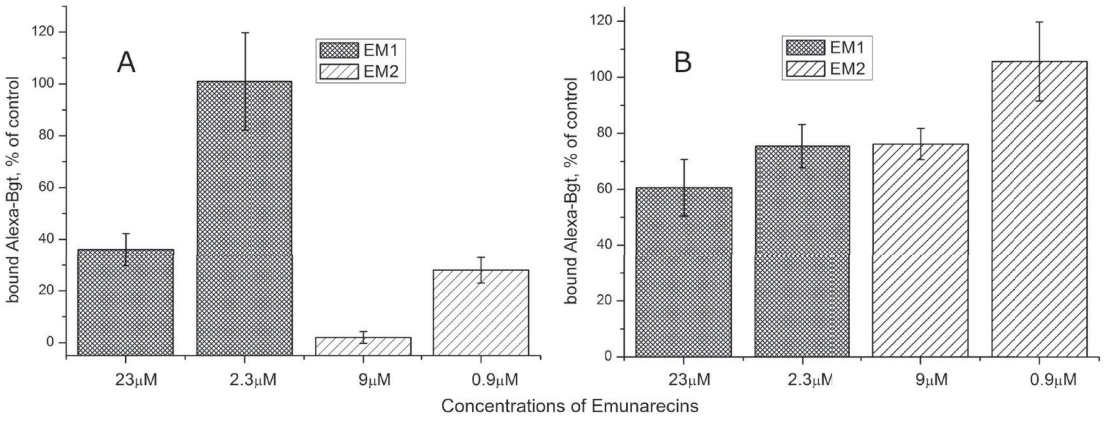

Figure 2. Competition of emunarecins with Alexa-Bgt for binding to the muscle type (A) and α7 (B) nAChRs. Alexa-Bgt, α-bungarotoxin labelled with Alexa 488; EM1, emunarecin 1; EM2, emunarecin 2. The data are presented as mean ±SEM.

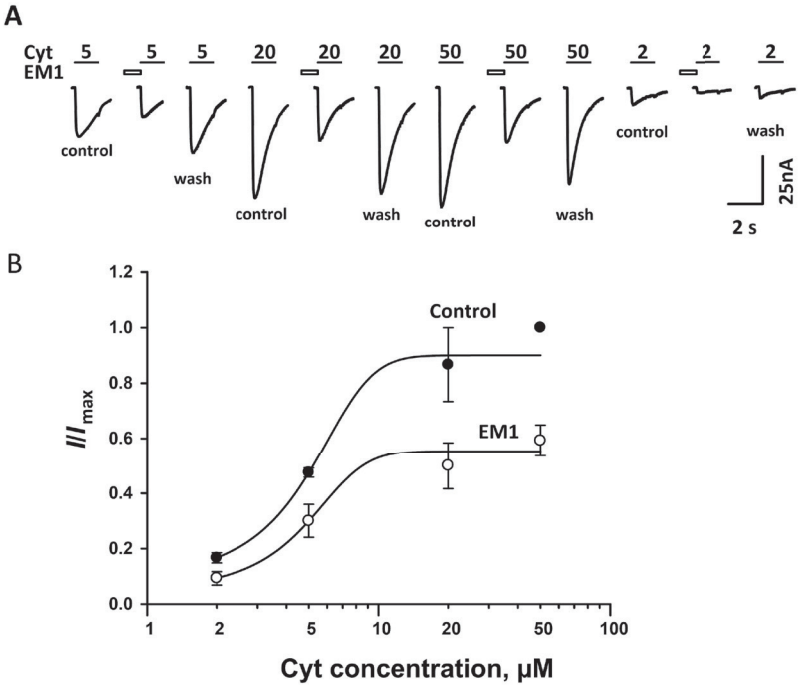

Figure 3. Inhibition of cytisine (Cyt)-elicited current by EM1 in *Lymnaea* neurons. (**A**) Representative traces of a neuron current responses to cytisine at four different concentrations before EM1 (100μg/ml) exposure (control), just after 5min exposure, and after 15min washing out. Cytisine concentrations in μM are shown above the horizontal bars indicating the duration of cytisine pulses. (**B**) Dependence of the current on cytisine concentrations in control (filled circles) and after treatment with EM1 at concentration of 100μg/ml (open circles). EC50 value for cytisine was not changed significantly (4.7μM in control and 4.8μM after EM1). Hill slope was 1.70 in control and 1.88 after EM1. Number of cells were from 3 to 5 for different cytisine concentrations. The data are presented as mean ±SEM.

with EM1 at a constant concentration of 100μg/ml. After 5min neuron treatment with 100μg/ml EM1, the response to a saturating cytisine concentration was decreased to 58%. At the same time there was no significant change in EC_{50} for cytisine: 4.8μM after exposure to EM1 versus 4.7μM in control (Figure 3B). These data suggest a non-competitive type of the receptor inhibition.

The value of IC_{50} for EM2 in inhibiting *Lymnaea* nAChRs (1.55μM) is in good agreement with the results obtained in this work on the muscle type nAChR . At the concentration of 1μM, EM2 inhibited Alexa-Bgt binding by 82% while at 9μM, the inhibition was almost complete. At the same time, the results for the interaction of EMs with human α7 nAChR are different from those obtained on the *Lymnaea* neurons. So, the emunarecins inhibited the currents elicited by agonists in snail nAChRs, but very weak competition with Alexa-Bgt for binding to human α7 nAChR was observed in this work. This dissimilarity may be explained by differences in the pharmacological and biophysical properties between *Lymnaea* and α7 nAChRs. First of all, unlike vertebrate receptors, nAChRs in *Lymnaea* neurons studied are chloride-conducting ion channels. In addition, there are two subtypes of *Lymnaea* nAChR, differing in sensitivity to α-conotoxin ImI and in the current kinetics (Vulfius et al, 2005), both nAChR subtypes controlling chloride conductance (Gorbacheva et al, 2018). Qualitative differences were also found in the sensitivity to different ligands between *Lymnaea* and α7 nAChRs as well as between the two *Lymnaea* subtypes. For example, the EC_{50} for acetylcholine in *L. stagnalis* neurons was 2-3μM versus 80-180*μM in* the vertebrate α7 nAChRs (Bertrand et al, 1992; Albuquerque et al, 1997, Criado et al, 2012). The IC_{50} for inhibition of the agonist-induced current by ImI was about 10nM for one nAChR subtype and 300nM for another, whereas it varied from 85 to 600nM in vertebrate α7 nAChR depending on the animal species (Johnson et al, 1995; Pereira et al, 1996; López et al, 1998; Ellison et al, 2003, 2004). The difference in the affinity for emunarecins in *Lymnaea* and α7 nAChRs adds another distinction between these receptors. The weak competition of emunaricines with Alexa-Bgt at α7 nAChR might be also explained by their interaction with some binding site which does not overlap with that for Alexa-Bgt, *i.e.*, a classical nAChR orthosteric site. This suggestion is supported by a non-competitive type of EM1 antagonism at *Lymnaea* nAChRs observed in electrophysiological experiments. It can be assumed that binding of the emunarecin in some allosteric site of the receptor prevents opening of the channel induced by the agonist but weakly interferes with α-Bgt binding to the orthosteric site. Very similar results were obtained with α-conotoxin ImII at human α7 nAChRs in inhibiting the acetylcholine-elicited current but not competing with α-Bgt for binding (Ellison et al, 2004).

The efficiency of EM2 interaction with muscle-type nAChRs was comparable to that of some neurotoxins from cobra venoms. For example, a non-conventional toxin WTX from *Naja kaouthia* venom competed with radioactive α-Bgt for binding to the *T. californica* nAChR with an IC_{50} of 2.2μM (Utkin et al, 2001). In summary, we can conclude that the CTLPs are able to interact with the nAChRs.

CONCLUSIONS

The data obtained in this work indicate that C-type lectin-like proteins, which are among the main non-enzymatic components in viper venoms, are able to interact with vertebrate nAChRs. It was shown that CTLPs from the venom of the saw-scaled viper *E. multisquamatus* inhibited the binding of fluorescently labeled α-bungarotoxin to nAChR from *Torpedo* electric organ. Together with the data obtained earlier, these results are an indication that CTLPs may represent new ligands for various nAChRs.

ACKNOWLEDGEMENTS

The reported study was funded by RFBR according to the research project No 18-54-05012.

The authors thank Mr Denis Ivanov for the help with toxin binding experiments.

COMPETING INTERESTS

None declared.

LIST OF ABBREVIATIONS

Alexa-Bgt: α-Bungarotoxin labelled with Alexa 488
α-Bgt: α-Bungarotoxin
CTLP: C-type lectin like protein
EM: emunarecin
nAChR: nicotinic acetylcholine receptor

REFERENCES

Albuquerque EX, Alkondon M, Pereira EFR, et al. 1997. Properties of neuronal nicotinic acetylcholine receptors: pharmacological characterization and modulation of synaptic function. J Pharmacol Exp Therap, 280, 1117-1136.

Arlinghaus FT, and Eble JA. 2012. C-type lectin-like proteins from snake venoms. Toxicon, 60, 512-519.

Bertrand D, Bertrand S, and Ballivet M. 1992. Pharmacological properties of the homomeric α7 receptor. Neurosci Lett, 146, 87-90.

Casewell NR, Harrison RA, Wüster W, Wagstaff SC. 2009. Comparative venom gland transcriptome surveys of the saw-scaled vipers (Viperidae: Echis) reveal substantial intra-family gene diversity and novel venom transcripts. BMC Genomics, 10, 564.

Cavalcante WLG, Noronha-Matos JB, Timóteo MA, Fontes MRM, Gallacci M, and Correia-de-Sá P. 2017. Neuromuscular paralysis by the basic phospholipase A2 subunit of crotoxin from Crotalus durissus terrificus snake venom needs its acid chaperone to concurrently inhibit acetylcholine release and produce muscle blockage. Toxicol Appl Pharmacol, 334, 8-17.

Criado M, Valor LM, Mulet J, Gerber S, Sala S, and Sala F. 2012. Expression and functional properties of α7 acetylcholine nicotinic receptors are modified in the presence of other receptor subunits. J Neurochem, 123, 504-514.

Deshimaru M, Ichihara M, Hattori T, Koba K, Terada S. 2005. Primary structure of brevilysin L4, an enzymatically active fragment of a disintegrin precursor from Gloydius halys brevicaudus venom. Toxicon, 45, 571-580.

Ellison M, McIntosh JM, and Olivera BM. 2003. α-Conotoxins ImI and ImII. Similar α7 nicotinic receptor antagonists act at different sites. J Biol Chem, 278, 757-764.

Ellison M, Gao F, Wang H-L, Sine SM, McIntosh JM, and Olivera BM. 2004. α-Conotoxins ImI and ImII target distinct regions of the human α7 nicotinic acetylcholine receptor and distinguish human nicotinic receptor subtypes. Biochemistry, 43, 16019-16026.

Gorbacheva EV, Starkov VG, Tsetlin VI, Utkin YuN, and Vulfius CA. 2008. Viperidae snake venoms block nicotinic acetylcholine receptors and voltage-gated Ca2+ channels in identified neurons of fresh-water snail *Lymnaea stagnalis*. Biochemistry (Moscow) Supplement Series A: Membrane and Cell Biology, 2, 14-18.

Gorbacheva EV, Ershova VS, Astashev ME, and Vulfius CA. 2018. Two subtypes of nicotinic acetylcholine receptors in *Lymnaea stagnalis* neurons control chloride conductance. Biochemistry (Moscow) Supplement Series A: Membrane and Cell Biology, 12, 261-267.

Johnson DS, Martinez J, Elgoyhen AB, Heinemann SF, and McIntosh JM. 1995. α-Conotoxin ImI exhibits subtype-specific nicotinic acetylcholine receptor blockade: preferential inhibition of homomeric α7 and α9 receptors. Mol Pharmacol, 48, 194-199.

López MG, Montiel C, Herrero CJ et al. 1998. Unmasking the functions of the chromaffin cell α7 nicotinic receptor by using short pulses of acetylcholine and selective blockers. Proc Natl Acad Sci USA, 95, 141841-141849.

Ma B, Zhang K, Hendrie C, et al. 2003. PEAKS: powerful software for peptide de novo sequencing by tandem mass spectrometry. Rapid Communications in Mass Spectrometry, 17, 2337-2342.

Madeira F, Park YM, Lee J, et al. 2019. The EMBL-EBI search and sequence analysis tools APIs in 2019. Nucleic Acids Res, 47, W636-W641.

Pereira EF, Alkondon M, McIntosh JM, and Albuquerque EX. 1996. Alpha-conotoxin-ImI: a competitive antagonist at alpha-bungarotoxin-sensitive neuronal nicotinic receptors in hippocampal neurons. J Pharmacol Exp Ther, 278, 1472-1483.

Petrova SD, Atanasov VN, and Balashev K. 2012. Vipoxin and its components: structure-function relationship. Adv Protein Chem Struct Biol, 87, 117-153.

Ramazanova AS, Zavada LL, Starkov VG, et al. 2008. Heterodimeric neurotoxic phospholipases A2--the first proteins from venom of recently established species *Vipera nikolskii*: implication of venom composition in viper systematics. Toxicon, 51, 524-537.

Rappsilber J, Mann M, and Ishihama Y. 2007. Protocol for micro-purification, enrichment, pre-fractionation and storage of peptides for proteomics using StageTips. Nature Protocols, 2, 1896-1906.

Sampaio SC, Hyslop S, Fontes MR, et al. 2010. Crotoxin: novel activities for a classic beta-neurotoxin. Toxicon, 55, 1045-1060.

Utkin YN, Kukhtina VV, Kryukova EV, et al. 2001. "Weak toxin" from *Naja kaouthia* is a nontoxic antagonist of alpha 7 and muscle-type nicotinic acetylcholine receptors. J Biol Chem, 276, 15810-15815.

Utkin YN, Weise C, Kasheverov IE, et al. 2012. Azemiopsin from *Azemiops feae* viper venom, a novel polypeptide ligand of nicotinic acetylcholine receptor. J Biol Chem, 287, 27079-27086.

Van de Velde AC, Gay CC, Moritz MNO, Dos Santos PK, Bustillo S, Rodríguez JP, Acosta OC, Biscoglio MJ, Selistre-de-Araujo HS, Leiva LC. 2018. Purification of a fragment obtained by autolysis of a PIIIb-SVMP from Bothrops alternatus venom. Int J Biol Macromol, 113, 205-211.

Vulfius CA, Krasts IV, Utkin YuN, and Tsetlin VI. 2001. Nicotinic receptors in *Lymnaea stagnalis* neurons are blocked by α-neurotoxins from cobra venoms Neurosci Lett, 309, 189-192.

Vulfius CA, Tumina OB, Kasheverov IE, Utkin YN, and Tsetlin VI. 2005. Diversity of nicotinic receptors mediating Cl- current in *Lymnaea* neurons distinguished with specific agonists and antagonist. Neurosci Lett, 373, 232-236.

Vulfius CA, Kasheverov IE, Starkov VG, et al. 2014. Inhibition of nicotinic acetylcholine receptors, a novel facet in the pleiotropic activities of snake venom phospholipases A2. PLoS One, 9, e115428.

Vulfius CA, Starkov VG, Andreeva TV, Tsetlin VI, and Utkin YN. 2015. Novel antagonists of nicotinic acetylcholine receptors-

proteins from venoms of Viperidae snakes. Dokl Biochem Biophys, 461, 119-122.
Vulfius CA, Spirova EN, Serebryakova MV, et al. 2016. Peptides from puff adder *Bitis arietans* venom, novel inhibitors of nicotinic acetylcholine receptors. Toxicon, 121, 70-76.
Vulfius CA, Kasheverov IE, Kryukova EV, et al. 2017. Pancreatic and snake venom presynaptically active phospholipases A2 inhibit nicotinic acetylcholine receptors. PLoS One, 12, e0186206.
Weinstein SA, Schmidt JJ, Bernheimer AW, and Smith LA. 1991. Characterization and amino acid sequences of two lethal peptides isolated from venom of Wagler's pit viper, Trimeresurus wagleri. Toxicon, 29, 227-236.
Yamada D, Sekiya F, and Morita T. 1996. Isolation and characterization of carinactivase, a novel prothrombin activator in *Echis carinatus* venom with a unique catalytic mechanism. J Biol Chem, 271, 5200-5207.
Yamada D, and Morita T. 1997. Purification and characterization of a Ca2+-dependent prothrombin activator, multactivase, from the venom of *Echis multisquamatus*. J Biochem, 122, 991-997.